Supplementary Material for Broadband Phonon Scattering in PbTe-based Materials Driven Near the Ferroelectric Phase Transition by Strain or Alloying

Ronan M. Murphy[1,2], Éamonn D. Murray[3], Stephen Fahy[1,2], and Ivana Savić[2]

[1] *Department of Physics, University College Cork, College Road, Cork, Ireland*

[2] *Tyndall National Institute, Dyke Parade, Cork, Ireland and*

[3] *Department of Physics and Department of Materials, Imperial College London, London SW7 2AZ, UK*

(Dated: March 2, 2016)

I. CALCULATION OF HARMONIC AND ANHARMONIC INTERATOMIC FORCE CONSTANTS

We used the Phono3py code [1, 2] to generate a minimal set of atomic displacements from which a full set of harmonic and third order anharmonic interatomic force constants (IFCs) can be reconstructed using lattice symmetries. To account for the long-range interatomic interaction in PbTe based materials [3], we imposed a cut-off on the interaction at 8 nearest neighbor shells (NNs) for anharmonic IFCs of PbTe, $PbSe_{0.5}Te_{0.5}$ and $Pb_{0.51}Ge_{0.49}Te$. We tested decreasing the range of anharmonic IFCs to 5 NNs, and found that this affected the lattice thermal conductivity by less than 5%. Subsequently, to decrease the computational load, we cut-off the interaction at 5 NNs for $Pb_{1-x}Ge_xTe$ alloys with $0 < x < 0.49$ and 10 NNs for strained PbTe and $PbSe_{0.5}Te_{0.5}$, which is equivalent to the 5 NNs cut-off in their equilibrium counterparts. The truncation of anharmonic IFCs breaks translational invariance of the crystal, which is enforced by identifying independent IFCs, and correcting them using a Lagrange multipliers technique [4] which maintains all symmetry properties of the crystal. We accounted for the long range ion-ion interaction by using an interpolation scheme at general $\mathbf{q}$ points with the non-analytical term correction [5]. We calculated the Born effective charges and dielectric constants using density functional perturbation theory as implemented in ABINIT [6].

II. VERIFICATION OF OUR APPROACH

To verify the validity of our approach, we calculated the phonon band structure and the lattice thermal conductivity κ of PbTe, and compared them with experiments. Harmonic and anharmonic IFCs of PbTe were calculated on supercells with 64 and 216 atoms, and we found that it is necessary to use 216 atoms supercells to obtain better convergence of the quantities of interest. Our computed phonon dispersion of PbTe is in good agreement with inelastic neutron scattering (INS) measurements of Cochran *et al.* [7], as illustrated in Fig. 1. In contrast, PbTe INS measurements of Delaire *et al.* [8] exhibit features that were ascribed to phonon-phonon interaction terms beyond the third order considered here. This indicates that our approach is more accurate for lower temperatures ($100 - 300$ K), where higher order anharmonic terms are less prominent.

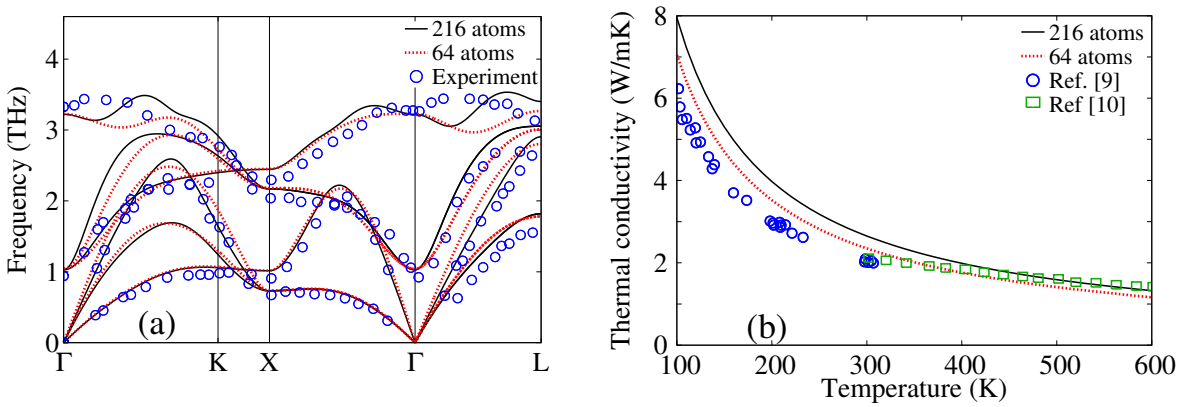

FIG. 1: (color online) (a) Phonon dispersions of PbTe: calculated using 216 atoms supercell at 0 K (solid black line), calculated using 64 atoms supercell at 0 K (dotted red line), and measured by Cochran *et al.* [7] at 300 K (blue circles). (b) Lattice thermal conductivity of PbTe as a function of temperature: calculated using a supercell with 216 atoms (solid black line), calculated using a supercell with 64 atoms (dotted red line), and measured by Devyatkova *et al.* [9] (blue circles) and by El-Sharkawy *et al.* [10] (green rectangles).

Our calculated κ of PbTe is $\sim 30\%$ larger than the experimental values obtained on undoped ($\sim 10^{17}$ cm^{-3}) single- and poly-crystalline PbTe samples using the absolute steady-state technique in the temperature range $100 - 300$ K [9], see Fig. 2. Since the κ of PbTe is very sensitive to the lattice constant changes within the accuracy of the DFT-LDA pseudopotential approach ($\sim 1\%$), we deem this agreement very good. We note that for conventional semiconducting materials, such as Si, Ge and SiGe alloys, our calculations are within $\sim 10\%$ of experimental values. On the other hand, our calculated κ of PbTe is in better agreement with the κ measured on undoped poly-crystalline PbTe samples using the plane temperature waves technique for temperatures $300 - 600$ K [10], see Fig. 2. This improved agreement may be somewhat fortuitous, since the departure of the measured κ values from the $\sim T^{-1}$ dependence for temperatures larger than 300 K may be due to stronger higher order anharmonic terms, as argued in Ref. [11].

III. SOFT TRANSVERSE OPTICAL MODES AND PHONON SCATTERING

To understand the role of soft transverse optical (TO) modes in inducing efficient phonon scattering for the materials driven near the ferroelectric phase transition, we calculated

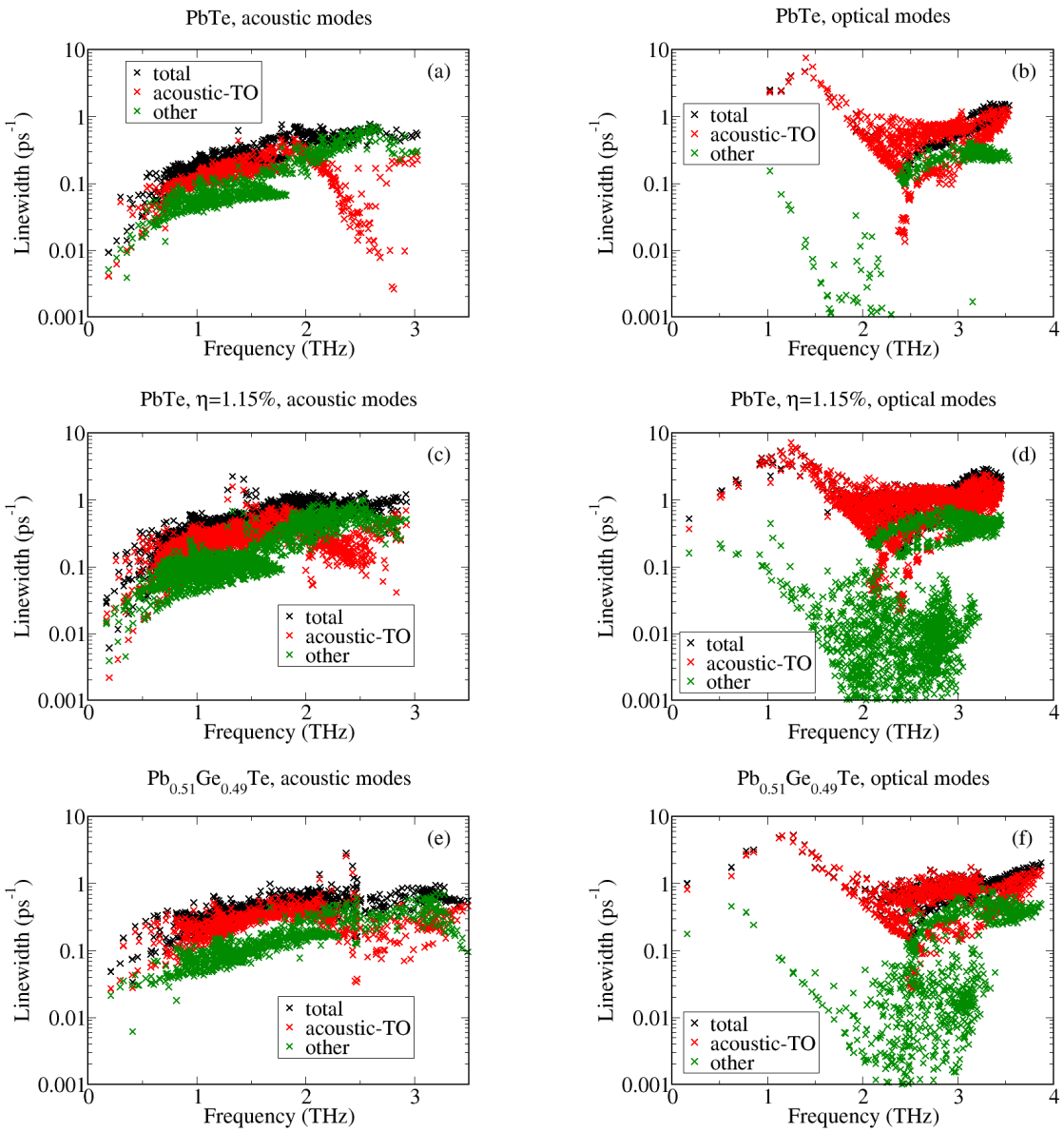

FIG. 2: (color online) The total anharmonic linewidth at 300 K as a function of frequency (black crosses) together with its contribution from the scattering processes that involve both acoustic and transverse optical (TO) modes (red crosses) and the contribution from all other scattering processes (green crosses) for (a) acoustic modes in PbTe, (b) optical modes in PbTe, (c) acoustic modes in strained PbTe, (d) optical modes in strained PbTe, (e) acoustic modes in $Pb_{0.51}Ge_{0.49}Te$, and (f) optical modes in $Pb_{0.51}Ge_{0.49}Te$. The acoustic-TO contribution to the anharmonic linewidth dominates over the other contributions in all these materials.

explicitly the acoustic-TO contribution to the total anharmonic linewidth in PbTe, strained PbTe and $Pb_{0.51}Ge_{0.49}Te$ at 300 K, shown in Fig. 2. This contribution was computed for all phonon frequencies by accounting for the triplets of interacting states that contain at least one acoustic and one TO mode. For each wave vector, we labeled the two lowest phonon modes as transverse acoustic (TA) modes, and the highest mode as longitudinal optical (LO) mode. Since the ordering of TO and longitudinal acoustic (LA) modes changes throughout the Brillouin zone, we distinguished between them using the following procedure. We determined which one of those three states is mostly longitudinal by projecting their eigenvectors onto the corresponding wave vector, and classified it as LA mode, while the other two states were labeled as TO modes. We found that the acoustic-TO contribution to the anharmonic linewidth dominates over the other contributions across the spectrum in both equilibrium and strained PbTe. It accounts for $\sim 70\%$ of the anharmonic linewidth of acoustic and LO modes (except for the $\sim 2-3$ THz range), and for nearly 100% of the anharmonic linewidth of TO modes (see Fig. 2). Furthermore, by driving PbTe near the phase transition, the acoustic-TO contribution to the anharmonic linewidth typically increases by a factor of $2-3$ throughout the spectrum, and up by a factor of $10-100$ for some frequencies. This is illustrated in Fig. 3 by comparing these contributions for strained PbTe and $Pb_{0.51}Ge_{0.49}Te$ to that of PbTe. We conclude that extremely soft TO modes generated by driving PbTe near the phase transition considerably increase the anharmonic acoustic-TO interaction, which in turn substantially reduces the phonon lifetimes.

To illustrate how soft TO modes close to the zone center affect phonon scattering in the materials near the phase transition, we calculated the contribution to the anharmonic linewidth due to the coupling of acoustic modes with the TO modes within the sphere centered at Γ with the radius of 1/3 of the Γ-X distance ($\sim 1/27$ volume of the Brillouin zone), here labeled as TO_1 modes. Our results for PbTe, strained PbTe and $Pb_{0.51}Ge_{0.49}Te$ at 300 K are illustrated in Fig. 4. Even though TO_1 modes contribute to only $\sim 1.3\%$ of the total number of modes, the acoustic-TO_1 contribution accounts for $\sim 20-30\%$ of the anharmonic linewidth throughout the spectrum, and for $\sim 100\%$ of the anharmonic linewidth of TO_1 modes. Additionally, by driving PbTe close to the phase transition via strain and alloying with GeTe, the acoustic-TO_1 contribution to the anharmonic linewidth typically increases by a factor of $2-3$ across the spectrum, and up by a factor of 10^2-10^7 for some frequencies, as shown in Fig. 5. These findings reveal an important contribution of

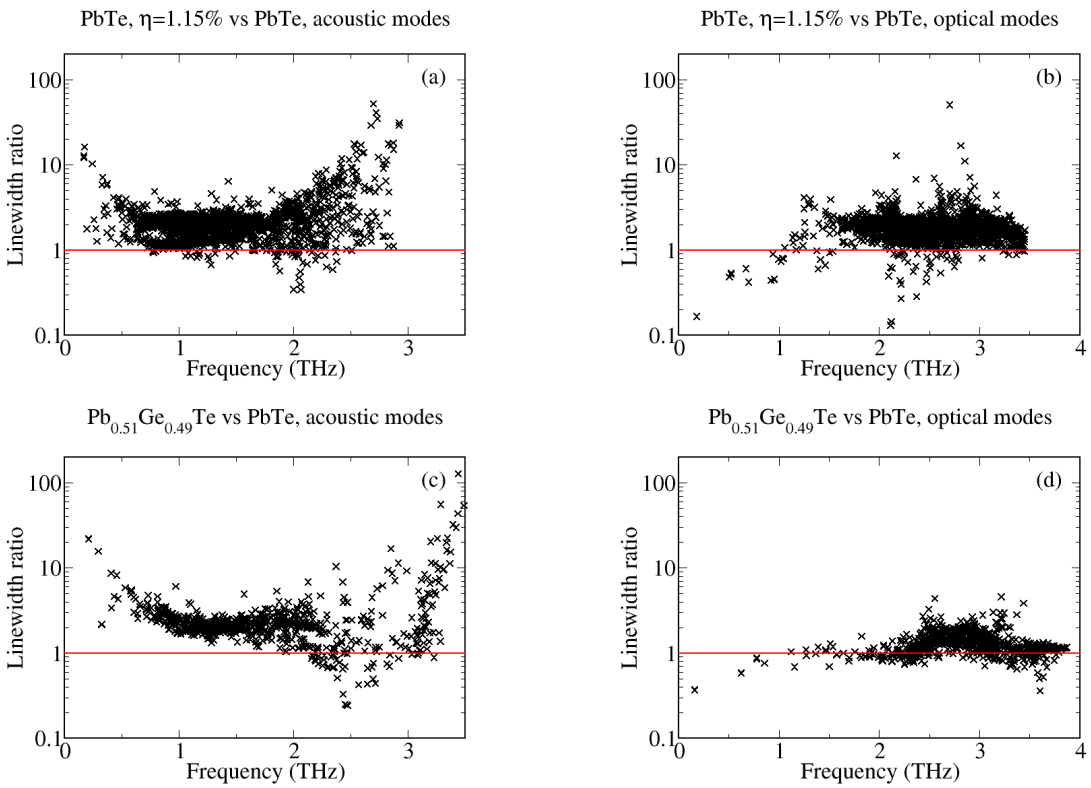

FIG. 3: (color online) The ratio of the acoustic-transverse optical (TO) contribution to the total anharmonic linewidth of strained PbTe and $Pb_{0.51}Ge_{0.49}Te$ with respect to PbTe at 300 K versus mode frequency of strained PbTe and $Pb_{0.51}Ge_{0.49}Te$, respectively. (a) Acoustic modes in strained PbTe, (b) optical modes in strained PbTe, (c) acoustic modes in $Pb_{0.51}Ge_{0.49}Te$, and (d) optical modes in $Pb_{0.51}Ge_{0.49}Te$. The acoustic-TO contribution to the anharmonic linewidth of the materials driven near phase transitions is larger than that of PbTe.

extremely soft TO modes close to Γ in increasing the anharmonic acoustic-TO interaction and reducing the phonon lifetimes in PbTe materials near the phase transition.

IV. THREE-PHONON SCATTERING VERSUS MASS DISORDER

Figs. 6 (a) and (b) show the three-phonon and mass disorder contributions to the phonon lifetimes at 300 K as a function of frequency in strained $PbSe_{0.5}Te_{0.5}$ and $Pb_{0.51}Ge_{0.49}Te$ alloy, respectively. Mass disorder is more efficient in scattering high-frequency phonons than three-phonon scattering, which results in an additional decrease of the phonon lifetimes at high frequencies and the lower κ of these materials compared to strained PbTe.

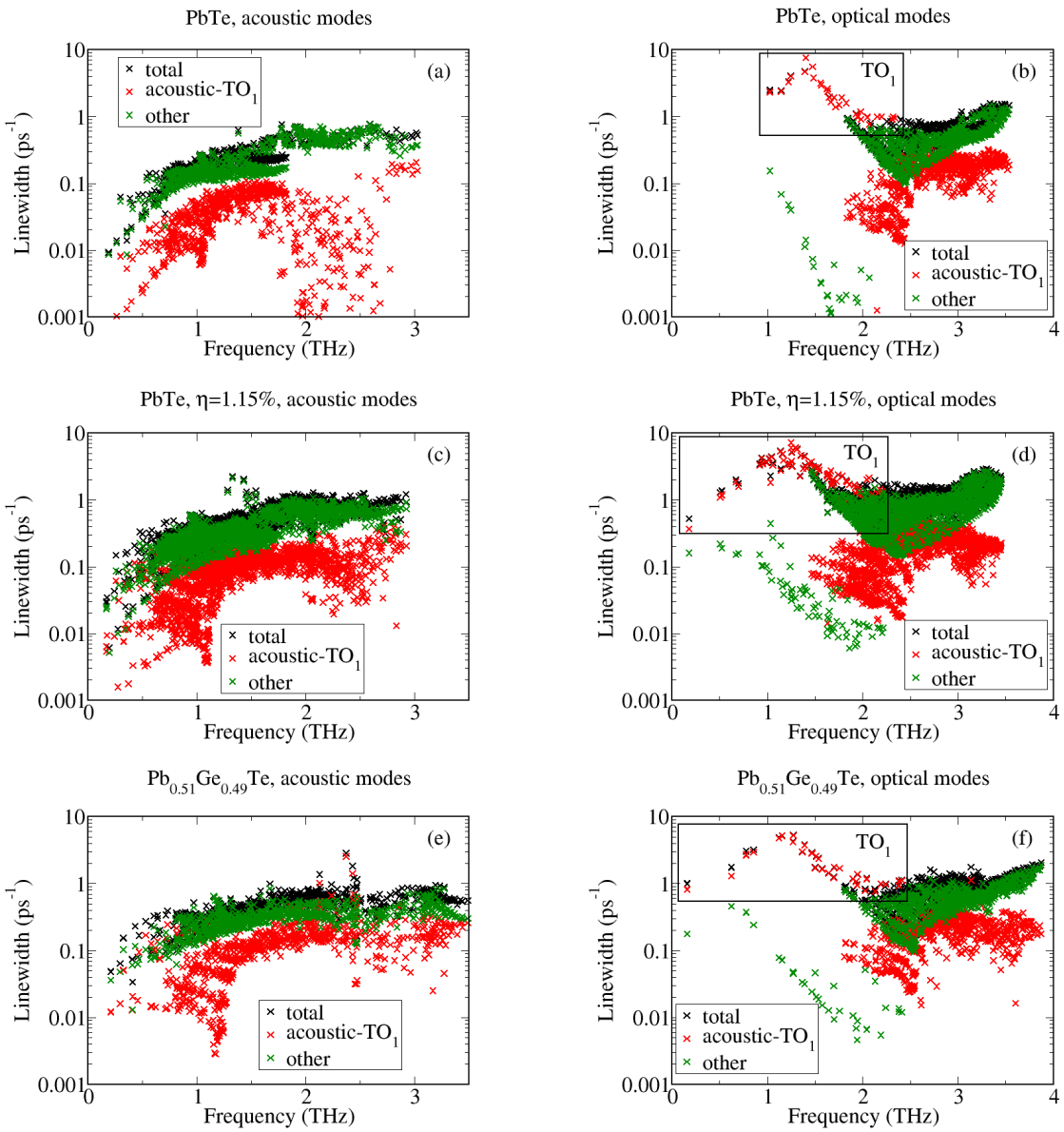

FIG. 4: (color online) The total anharmonic linewidth at 300 K as a function of frequency (black crosses) together with its contribution from the scattering processes that involve both acoustic and transverse optical modes close to the zone center (labeled as TO_1 modes, see text for explanation) (red crosses) and the contribution from all other scattering processes (green crosses) for (a) acoustic modes in PbTe, (b) optical modes in PbTe, (c) acoustic modes in strained PbTe, (d) optical modes in strained PbTe, (e) acoustic modes in $Pb_{0.51}Ge_{0.49}Te$, and (f) optical modes in $Pb_{0.51}Ge_{0.49}Te$. The frequencies of TO_1 modes correspond to red crosses within black boxes. The acoustic-TO_1 contribution represents a considerable fraction of the anharmonic linewidth in all these materials.

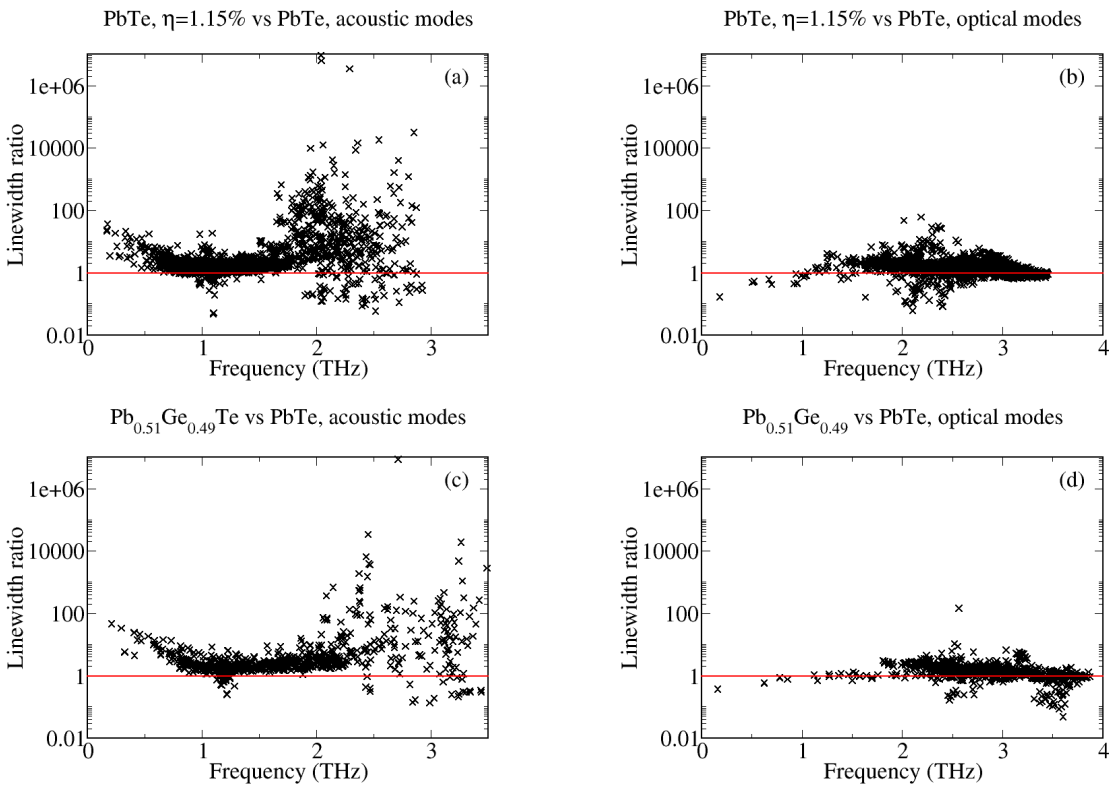

FIG. 5: (color online) The ratio of the acoustic-transverse optical modes close to the zone center (labeled as TO_1 modes, see text for explanation) contribution to the total anharmonic linewidth of strained PbTe and $Pb_{0.51}Ge_{0.49}Te$ with respect to PbTe at 300 K versus mode frequency of strained PbTe and $Pb_{0.51}Ge_{0.49}Te$, respectively. (a) Acoustic modes in strained PbTe, (b) optical modes in strained PbTe, (c) acoustic modes in $Pb_{0.51}Ge_{0.49}Te$, and (d) optical modes in $Pb_{0.51}Ge_{0.49}Te$. The acoustic-TO_1 contribution to the anharmonic linewidth of the materials driven near phase transitions is larger than that of PbTe.

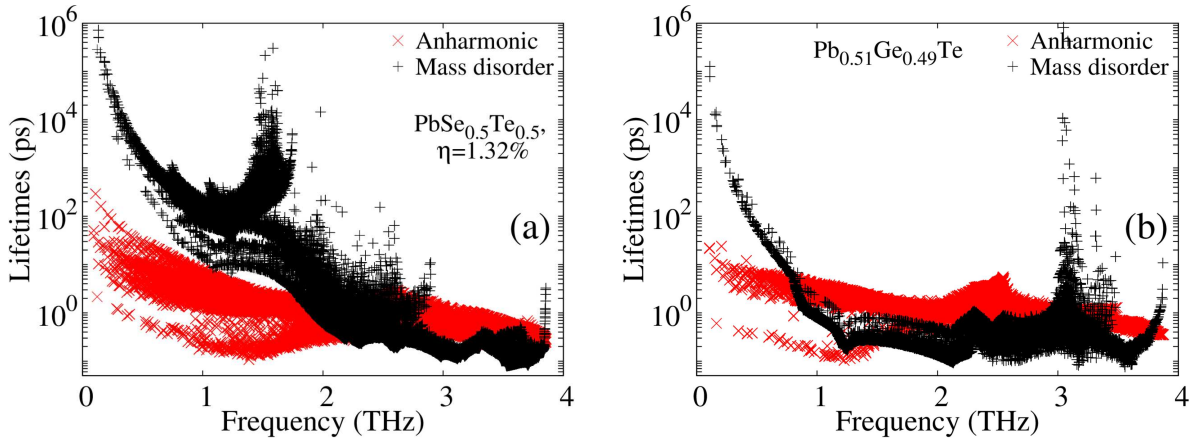

FIG. 6: (color online) Frequency dependence of the mass disorder and three-phonon contributions to the phonon lifetimes at 300 K (black pluses and red crosses, respectively) of (a) $PbSe_{0.5}Te_{0.5}$ driven near the phase transition by tensile [001] strain of $\eta = 1.32\%$, and (b) $Pb_{0.51}Ge_{0.49}Te$ alloy at the verge of the phase transition.

[1] A. Togo, F. Oba, and I. Tanaka, Phys. Rev. B **78**, 134106 (2008).

[2] L. Chaput, A. Togo, I. Tanaka, and G. Hug, Phys. Rev. B **84**, 094302 (2011).

[3] S. Lee, K. Esfarjani, T. Luo, J. Zhou, Z. Tian, and G. Chen, Nat. Comm. **5**, 3525 (2014).

[4] W. Li, L. Lindsay, D. A. Broido, D. A. Stewart, and N. Mingo, Phys. Rev. B **86**, 174307 (2012).

[5] Y. Wang, J. J. Wang, W. Y. Wang, Z. G. Mei, S. L. Shang, L. Q. Chen, and Z. K. Liu, J. Phys.: Condens. Matter **22**, 202201 (2010).

[6] X. Gonze and C. Lee, Phys. Rev. B **55**, 10355 (1997).

[7] W. Cochran, R. A. Crowley, G. Dolling, and M. M. Elcombe, Proc. R. Soc. Lond. A **293**, 433 (1966).

[8] O. Delaire, J. Ma, K. Marty, A. F. May, M. A. McGuire, M.-H. Du, D. J. Singh, A. Podlesnyak, G. Ehlers, M. D. Lumsden, et al., Nat. Mater. **10**, 614 (2011).

[9] E. D. Devyatkova and I. A. Smirnov, Sov. Phys. Solid State, USSR **3**, 1666 (1962).

[10] A. A. El-Sharkawy, A. M. A. El-Azm, M. I. Kenawy, A. S. Hillal, and H. M. Abu-Basha, Int. J. Thermophys. **4**, 261 (1983).

[11] A. H. Romero, E. K. U. Gross, M. J. Verstraete, and O. Hellman, Phys. Rev. B **91**, 214310 (2015).